UNIVERSITÀ DEGLI STUDI DI PADOVA
Dipartimento di Ingegneria Industriale

14

LiftUP Team

University of Padua

Air Cargo Challenge Report

Air Cargo Challenge 2019

Table of Contents

Introduction

This report summarizes the design of the small remote-controlled cargo aircraft designed by a team of students from the University of Padua (Italy), aiming to compete in the Air Cargo Challenge 2019 in Stuttgart (Germany). The team was founded in 2018 under supervision of professor Francesco Picano and is still growing in members: as of now, 22 students have joined.

This document reviews and describes our team's work from the first phases of design to the flying of the aircraft. Being this our first participation to the Air Cargo Challenge, we lacked any prior knowledge about the design processes and the construction methods required to build an aircraft, therefore extensive and in-depth studies had to be made prior to the establishment of the plane's main features; on the same note, no one had first-hand experience about the construction of model aircrafts. This led to the decision of building an early prototype in order to master the tools and techniques needed to design and build the final aircraft.

In the end, our team opted for a high single-wing aircraft with a V-shaped tailplane and a spring leaf taildragger landing gear, with the cargo bay located inside the fuselage. The first conceptual design came from the analysis of previous ACC competitions, from which we got ideas for the general shape of the aircraft. Then, the design was optimized with the help of various engineering softwares. When the design had been polished enough, we built our prototype to validate our calculations to find (and fix) any unexpected critical issues.

Project management

Organization chart and roles

In the early stages of the project's history, up until we reached a clear enough understanding of what had to be achieved, no major roles were given to team members, as everyone had yet to research and learn the many topics needed to build the final aircraft. Up to that point, the only established role was that of the team manager, who supervised everyone's work and kept track of expenses, and everyone's work was shared on a common folder on the cloud. Later on, as more people joined the team, it became clear that we needed a better workspace and a more hierarchic line of management. Thus, we chose to split the team into departments, with one person in charge of each one, and to assign specific roles to certain people.

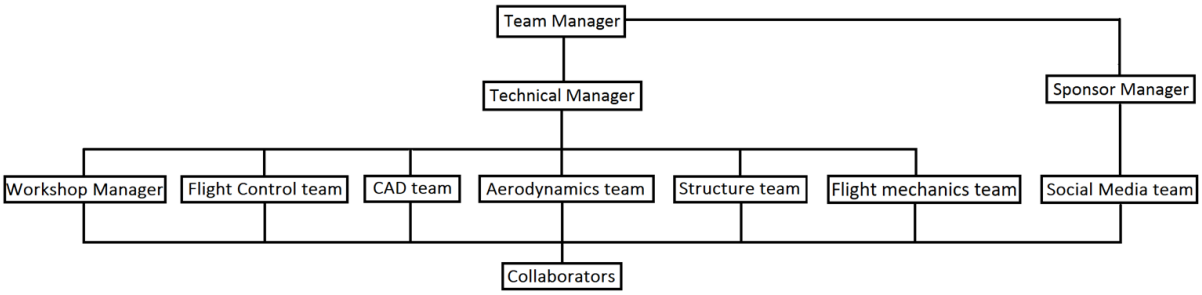

Figure 1: Organization chart

Team manager: administrates and organizes the team's work. His job is to establish a work plan for each group, to ensure that deadlines are followed and to manage the project's finances.
Technical manager: oversees the work done by each group and advises the team manager on how to overcome any technical issues. Along with the team manager, the technical manager leads the design and construction of the aircraft.
Aerodynamic Design team: is in charge of the shape of the aircraft. Their job is to size the main aerodynamic surfaces (wings, fuselage, etc) and evaluate the feasibility of possible performance-enhancing features (winglets, vortex generators, etc).
Structural Design team: designs the structures of the whole aircraft trying to stay as close as possible to the aerodynamic design, ensuring it will not fail under the predicted loads.
CAD team: keeps track of design changes and updates 2D and 3D models of the aircraft.
Flight Mechanics team: studies the flight pattern of the aircraft, its attitude during manoeuvres and changes the design in order to respect the rules of the competition.
Electronics team: chooses electrical components and is also in charge of the correct functioning of electronic mechanisms and radio controls.
Social media team: manages the project's website and social media accounts, in order to gain a good reputation and visibility with the general public and to grow the team's links with possible sponsors and companies.
Sponsor Manager: stays in contact with companies and researches funds for the project.
Workshop Manager: organizes work sessions and is in charge of tidying up the workspace, keeping track of tools and ensures that safety rules are always followed.
Collaborators: the remaining members of the team, who are not linked to any department.

They are free to choose their jobs and once an activity is over they can move from a group to another (if needed).

Work and time schedules

Since LiftUP is a team composed by students, its members are not always available at any given time. To overcome this problem, we shared virtual workspaces to let people work together without needing to physically meet. We based our main activities on Slack, a web-based platform organized in channels that let us share files and discuss issues without losing track of them over time. We also shared a Google Drive folder, in which we kept all files related to our project so that we could work on the same shared documents. For news and announcements we used Telegram, an instant messaging platform.

During the design phase we ruled that group managers, along with the team manager and collaborators, had to meet once a week on a designated day and time during lesson-free hours. Roughly once a month we also had meetings with our coordinating teacher to review the work done and show our results. Then, while building the prototype and the final aircraft, we established lab shifts and kept track of each member's work hours to ensure that groups could meet to build the subsystems of their responsibility.

Finances

The Lift Up project has been financed by the University of Padova receiving fundings for a total of 16500€. We wrote and sent a financial budget (the one on the right) to a competitive funding call of our University expecting an overall income of 15000€. We were confident that these funds would be granted since a big percentage of engineering projects are funded by the University and also because this year the University started an Aeronautical Engineering Master of Science program, showing its will to invest in the sector. From this funding call we got granted 11000€ in October; this wasn't a big issue, as we had 3000€ from a fund received in March 2018 by the Department of Industrial Engineering. This sum had to be used for building the 2017 regulation prototype. Since we never got to build the 2017 prototype we added this sum to the 2018/2019 budget covering almost all the expected outflow. The remaining 1000€ were not needed anymore as we did not have to get insurance for our pilot anymore. Following our request, on April 2019 the University granted us 2500€ more.

Financial budget September 2018	
Expected inflow	€ 15.000,00
Expected outflow	€ 15.000,00
Prototype	€ 3.000,00
Competition aircraft	€ 4.090,00
Advertising activity	€ 500,00
Workshop and tools	€ 2.000,00
Participation fee	€ 3.010,00
Pilot insurance	€ 900,00
Travel	€ 1.000,00

Figure 2: Financial budget of Sept. 2018

This prediction was almost right since the money outings so far are listed in the tables below.

Money outings 1 May 2019	
Prototype	€ 2.975,24
Competition aircraft	€ 2.971,18
Advertising activity	€ 7,00
Workshop and tools	€ 2.881,81
Participation fee	€ 3.010,00
Pilot insurance	€ 0,00
Travel	€ 0,00
Total outflow	€ 11.845,23

Expected outflows for the next months	
Expected inflow	€ 0,00
Expected outflow	€ 2.940,00
Prototype	€ 0,00
Competition aircraft	€ 1.100,00
Advertising activity	€ 240,00
Workshop and tools	€ 600,00
Participation fee	€ 0,00
Pilot insurance	€ 0,00
Travel	€ 1.000,00

Figure 3: Money outflows

We are keeping remaining funds for any unexpected inconveniences.

Sponsors and social media

LiftUP is sponsored by the *Department of Industrial Engineering*, which is part of the University of Padova; this main sponsor gave the funds and the workspace to the project. The team is also sponsored by G.A.F.T. (*Gruppo Aeromodellistico Frecce Tricolori*), which has offered the airfield for flight tests, *A.S. Euroavia Padova*, which started this project, *Academy Card Tech* and the *Maintenance service of the Padova Aeroclub*, which gave us the material used for the landing gear.

The LiftUP project has three main public communications channels: its website, Facebook and Instagram. The purpose of these channels is to show the progress of the team and to attract new members and sponsors.

Website: http://euroaviapadova.altervista.org/lift-up/
Facebook: https://www.facebook.com/LiftUP2018/
Instagram: https://www.instagram.com/liftup.padova/

Deadlines

Below is a list of the project activities in which we encountered difficulties, while the Gantt diagram with all the major activities is available on the following page.

Workshop setup: shelves and tools management to ensure a clean, productive working place. It suffered delays caused by late deliveries from tool suppliers and bureaucratic issues with our University.

Prototype construction: construction of prototype parts and assembly. It was delayed due to late workshop setup.
Prototype flight tests: tests on the prototype to find fixable issues. The number of tests was increased because of unfavourable meteorological conditions.
Infusion moulding tests: lamination tests for the fuselage. They have been delayed due to late delivery of materials from suppliers.

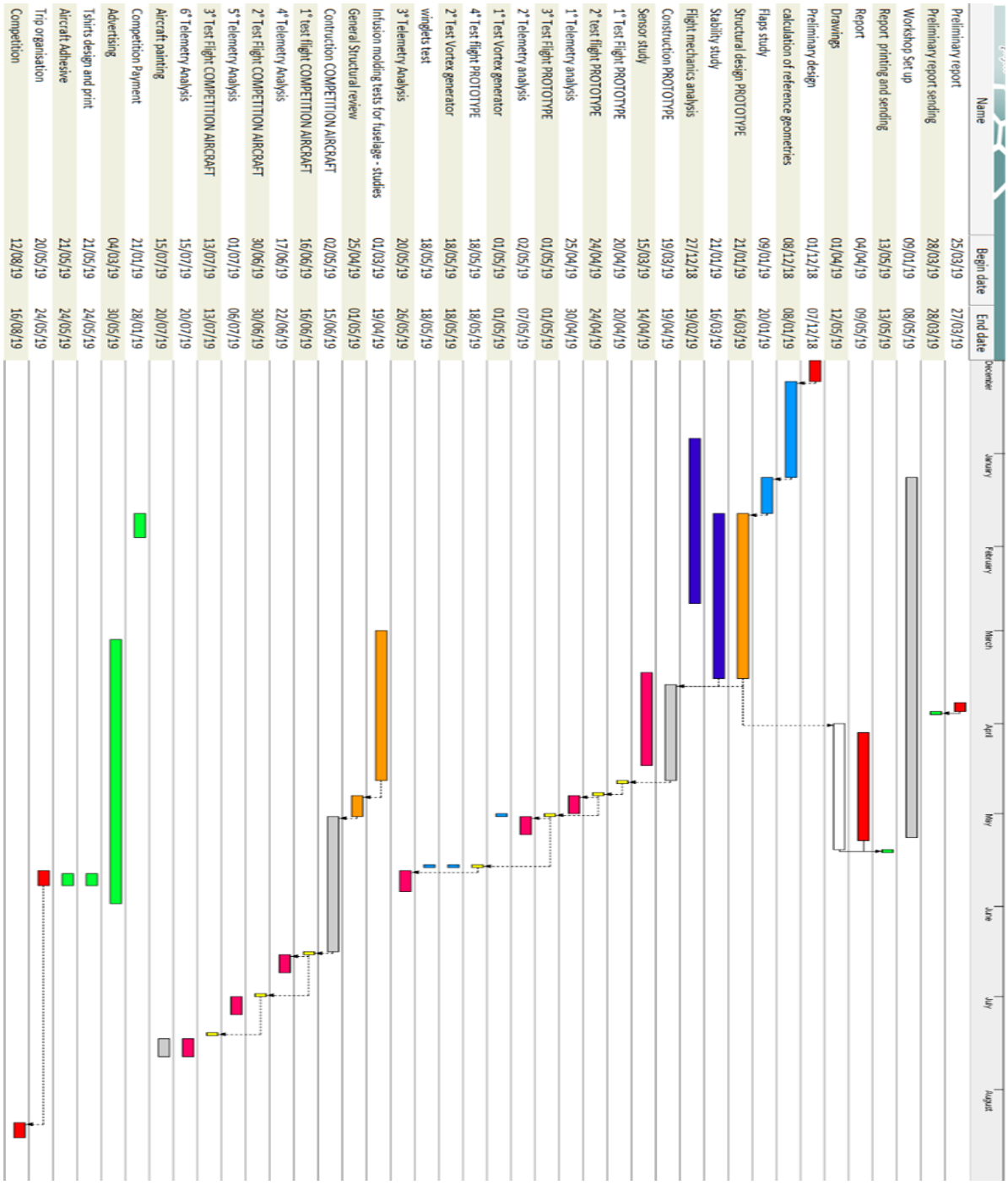

Figure 4: Gantt diagram and activities

Aerodynamic design

The main drivers for the aerodynamic design were the maximum take-off distance, the box dimensions and the payload capability. The team first focused on the wings, then on the tail stabilizer and, lastly, on the fuselage.

Wing design

The first step was to quantify motor and propeller performance. The analysis proceeded via software, using the eCalc performance tool on the AXI Gold 2826/10 motor and Aeronaut Cam Carbon light 12x7 propeller, required by the ACC 2019 rules. We used a MATLAB code to obtain the power available (P_A) in function of the airspeed and RPM of the motor, we used this data to define the aircraft take-off performance with the next simplified expression (we neglected ground friction and drag)

$$x_{takeoff} = \int_0^{V_{TO}} \frac{m \cdot V^2}{P_A} dV$$

Where g is the gravitational acceleration and V_{TO} is the takeoff speed. We also had to make an estimation of the total mass (m), which we couldn't know a priori. It was finally set at 11kg, based on previous editions of the ACC, considering that the transportation box is smaller and the propeller/motor have lower performances. Through the MATLAB code, we determined that the speed at the end of the 60m runway would be 12.2m/s.

From the speed and the approximate chord (assumed on the box size), we estimated the Reynolds number (*Re*=2.5e5) to start the airfoil choice process. As we do not have a wind tunnel at our disposal, while analysing a plethora of different airfoils taken from the UIUC catalogue, we only had to rely on numerical analysis with XFLR5 software, usually used for R/C planes design. The final choice was the SD7062 airfoil, picked for its high lift/drag ratio and simple geometry so as to make the production process easier (no pointy edges or too thin sections). Its coefficient of lift polar is shown below, where the curve highlighted is the one calculated for *Re*=2,5e5. Even though its maximum lift coefficient isn't extremely high ($C_{l,max}$=1,6), more performing airfoils in terms of lift were not chosen because their trailing edge was considered to be too pointy and thin to be built; also, we had already decided to fit the wing with flaps.

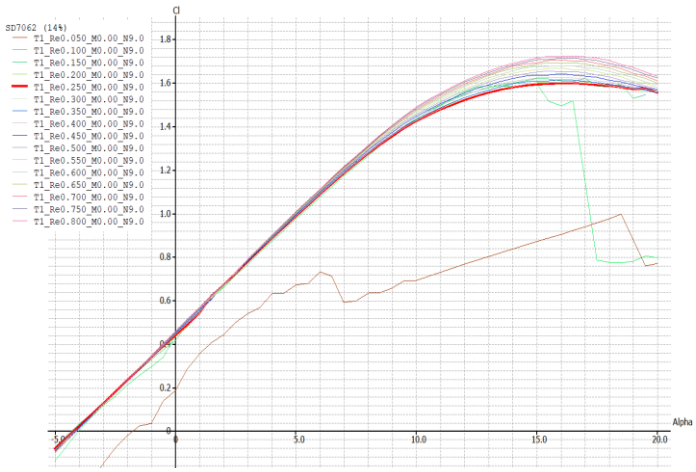

Figure 5: Lift coefficient polar curve

Using Prandtl's theory we estimated $C_{L,max}$=1,4 (assuming AR and$e$) and with the assumption $L = m \cdot g$, we got a wing surface of

$$S = \frac{2 \cdot m \cdot g}{\rho \cdot V_{TO}^2 \cdot C_{L,max}} = 0{,}9355 m^2$$

(ρ is the air density=1,225 kg/m^3 and $C_{L,max}$ is the maximum coefficient of lift the wing can provide without flap before stalling). The Aspect Ratio (AR) is set to 11 in order to fit the 5 sections of the wing inside the box,

with some margin for mountings and to leave some extra space for other components. The wingspan was then calculated to be $b = \sqrt{AR \cdot S}$=3,21m and the mean chord is c=S/b=0,29 m. Considering the fact that to calculate the take-off speed we did not consider any drag and ground friction, we did a second iteration of the design, by raising the wing surface to 1m^2 (to have some safety margin), while keeping AR=11. This slight change gave us back a wingspan b of 3,317m, mean chord c of 0,302m and it lets the plane take-off at a calculated speed of 11,24m/s. With this configuration each of the 5 wing sections is 0,663m long, so they still fit in the transportation box. We adopted a rectangular wing because it's easier to manufacture than tapered or elliptical wings.

Flaps and ailerons

To be sure that the plane will be able to take-off within 60 m we chose to fit flaps to the 3 central wing segments (the central segment has flap only for the 75% of the span). We opted for hinged flaps taking 30% of the chord, tilted by 20° for take-off and 30° for landing. We analysed the flapped airfoil in XFLR5, this analysis includes 5 different configurations of flaps between 0° (yellow curve) and 20° (red curve) at Re=3e5. Note that with a 20° configuration the maximum lift coefficient is about 1,9. We calculated the increase in the maximum wing's lift coefficient $\Delta C_{L,max}$ using the following formula

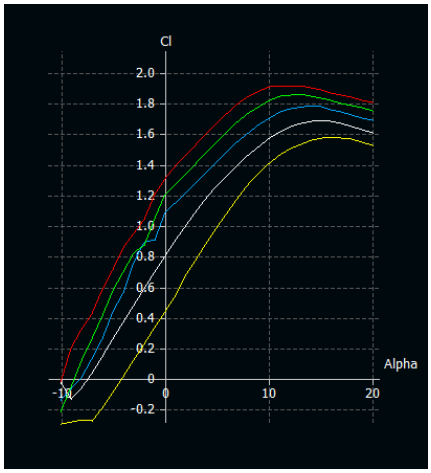

Figure 6: CL with differet flap configurations

$$\Delta C_{L,max} = \Delta C_{l,max} \cdot \frac{S_{flapped}}{S} = 0{,}18$$

This makes the $C_{L,max}$ of the flapped wing equal to 1,65.
For the ailerons, the same approach was used: 30% of the chord was used for the purpose along the whole width of the outer wing sections, and the deflection of the surface was 30° downward and 20° upward.

Angle of attack on take-off and cruise

When the aircraft lifts off the ground, we can approximate that its weight is balanced by the lift force, then we can write:

$$W = L = \frac{1}{2} \cdot \rho \cdot S \cdot C_{L,takeoff} \cdot v_{takeoff}^2$$

We can then calculate the lift coefficient at lift-off:

$$C_{L,takeoff} = \frac{2 \cdot W}{\rho \cdot S \cdot v_{takeoff}^2} = 1{,}3945$$

From Prandtl's theory we know that

$$C_{L,takeoff} = a \cdot (\alpha_{takeoff} - \alpha_{L=0}) = \frac{2 \cdot W}{\rho \cdot S \cdot v_{takeoff}^2}$$

Finally,

$$\alpha_{takeoff} = \frac{2 \cdot W}{\rho \cdot S \cdot v_{takeoff}^2 \cdot a} + \alpha_{L=0} = 11{,}92°$$

where a is the slope of the lift coefficient polar of the plane and $\alpha_{L=0}$is the angle of zero lift. In particular we calculated a with the next equation

$$a = \frac{a_0}{1 + \frac{a_0}{\pi e A R}}$$

Where $a_0$is the slope of the lift coefficient polar of the airfoil. Both $\alpha_{L=0}$and $a_0$were calculated from the polars obtained during the XFLR5 airfoil analysis shown in the *Wing design* section of this document.

The same calculations were made for cruise, in particular from the analysis of the other team's performance at ACC2017 the cruise speed was assumed to be 18 m/s, meaning a lift coefficient of $C_{L,cruise}$=0,5404 and α_{cruise}=2,08°.

Tail design

We started with the choice of the configuration (V-tail), then we made a preliminary dimensioning of the tail with the tail volume coefficients method, after that we made a stability analysis and we obtained the following final dimension: chord of 0,160m, half tail surface of 0,073m^2, half tail span of 0,516m, half tail aspect ratio of 3,65 and dihedral angle of 33,5°.

In particular we analysed three different configurations for the tail: conventional tail, T-tail and V-tail. A "V" shape configuration was chosen for the stabilizer for three main reasons:

- it's easier to design and lighter than a classical "T" configuration;
- It offers reduced wetted area and interference drag;

After choosing the tail configuration, we analysed multiple airfoils, especially symmetric ones, and we compared four of them: NACA0009, S9033, S9032 and HT14. We compared them with XFLR5 at Re=2,5e5, obtaining the following results:

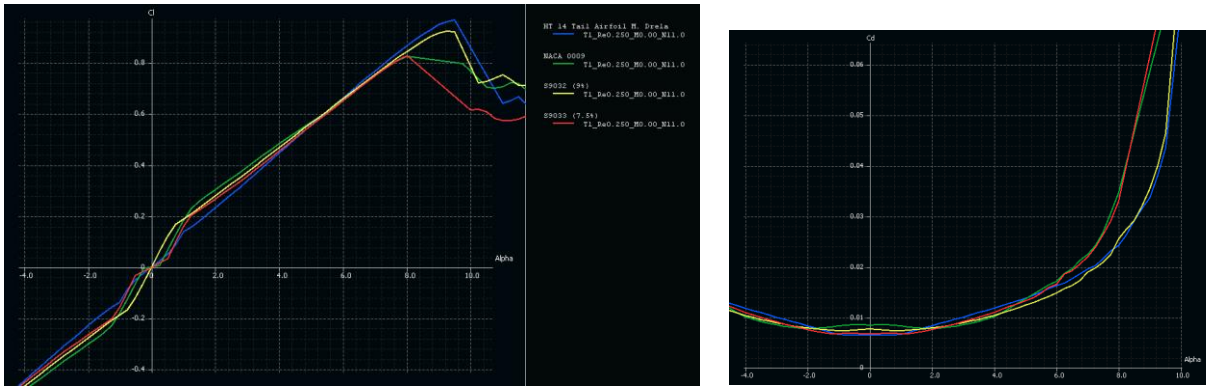

Figure 7: Comparison between different tail airfoils

These airfoils show similar behaviour of the lift coefficient and a similar maximum lift coefficient, but we can see that HT14 has a slightly lower drag coefficient at low angle and for this reason we picked the last one.

Using the "tail volume coefficient" method from Raymer's *Aircraft Design: A Conceptual Approach*, we made the preliminary sizing, the formulas for the horizontal and vertical surface

are:

$$S_{HT} = \frac{c_{HT} \cdot c \cdot S}{L_{HT}} \text{ and } S_{VT} = \frac{c_{VT} \cdot b \cdot S}{L_{VT}}$$

where C_{VT} and C_{HT} are coefficients specific for each aircraft typology; we assumed our plane to be most similar to a glider, so C_{VT}=0,02 and C_{HT}=0,50. Furthermore, we assumed L_{HT}=L_{VT}=L=0,9m, as to obtain S_{HT}=0,168m^2 and S_{VT}=0,074m^2. For the V tail (as written in *NACA report No.823*) the total surface area is the sum of the two, so $S_{V,tot}$=0,242m^2; each part of the tail will then have a surface of $S_{V/2}$=0,121m^2; their dihedral angle can be calculated through

$$\Gamma = \cos^{-1}\sqrt{\frac{S_{HT}}{S_{V,tot}}} = 33{,}5°.$$

Static stability analysis

The condition needed to have longitudinal static stability is that the slope of the longitudinal moment coefficient of the aircraft is negative, or

$$C_{M_\alpha} = \frac{\partial C_M}{\partial \alpha} < 0$$

The value of C_{M_α} depends on the static margin which determines the degree of stability of the aircraft, and to know the static margin it is also necessary to know the position of the centre of mass of the aircraft. For this reason, we estimated the distribution of the masses of our aircraft takes advantage of previous prototype knowledge, that is represented in the next figure.

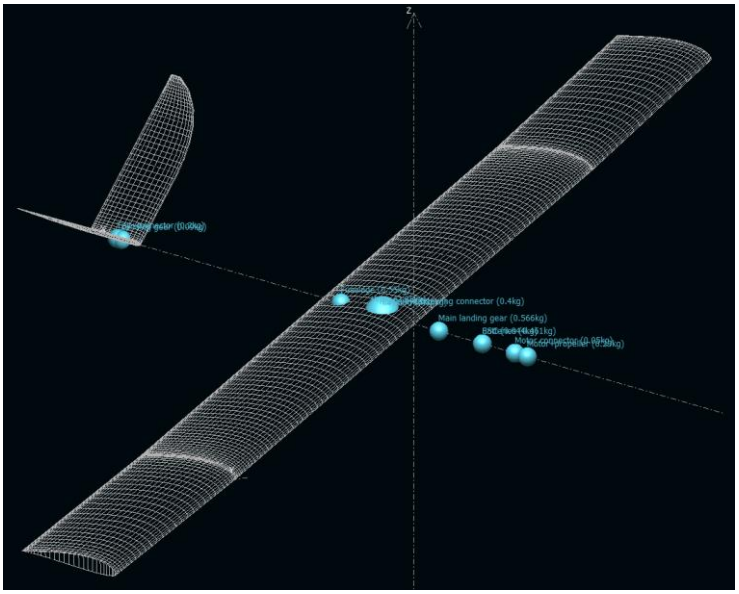

Figure 8: Distribution of masses

Starting from the preliminary geometry calculated for the tail (for each semi-wing: S=0,141m^2, b=0,756m, c=0,160m), we proceeded with the evaluation of 3 different configurations, in which we reduced the tail surface by 30%, 40% and 50% to highlight the influence of this surface on the aircraft stability. By fixing c=0,160m and applying the following formulas, we got the table below

$$b_{V/2} = \frac{S_{V/2}}{c} \text{(semi-tail's wingspan)}, \; AR_{V/2} = \frac{b_{V/2}^2}{S_{V/2}} \text{(semi-tail's aspect ratio)}$$

By modelling these configurations (together with the wing which was tilted at the cruise incidence (2,08°) respect the fuselage in order to have the fuselage aligned with the air flow during the cruise) in the XFLR5 software it was possible, through iterations, to calculate the incidence of the tail respect the fuselage (i_S) in order to maintain longitudinal equilibrium of the aircraft in cruise condition, which is reached when C_M=0. We could also calculate the static margin given by the different configurations as follows:

$$H_n = \frac{x_{pn}}{c} - \frac{x_{cg}}{c}$$

where c=0,302m (wing's mean chord), x_{cg} is the aircraft centre of mass position and x_{pn} is the position of the neutral point of the aircraft and it can be extrapolated from XFLR5 for every tail configuration. We found the following results:

Configuration	$S_{V/2}$	$b_{V/2}$	$AR_{V/2}$	i_S	H_n	$C_{M\alpha}$
1	0,121m^2	0,756m	4,72	0,41°	22,85%	-1,1179
2 (-30%)	0,085m^2	0,529m	3,30	-0,20°	12,25%	-0,5993
3 (-40%)	0,073m^2	0,454m	2,82	-0,60°	8,61%	-0,4212
4 (-50%)	0,061m^2	0,378m	2,34	-1,20°	4,97%	-0,2432

In which $C_{M\alpha}$was calculated with:

$$C_{M\alpha} = -a \cdot H_n$$

Where a is the slope of the lift coefficient of the aircraft and it could be approximated to the slope of the lift coefficient of the wing + tail. We can see from the pictures below that all configurations are stable ($C_{M\alpha} < 0$), we can also see that the aircraft is in equilibrium (C_M=0) when $\alpha = 0$ (where α is the incidence of the fuselage with respect to the air flow). The first configuration cannot be implemented as the tail would not fit in the box.

Through the software we could also compare the efficiency of the different configurations: configurations 3 and 4 are considerably more efficient than the others while number 1 is the most penalised. Moreover, from flight tests we saw that good values of the static margin are around 10%, so we chose configuration 3 for the final aircraft.

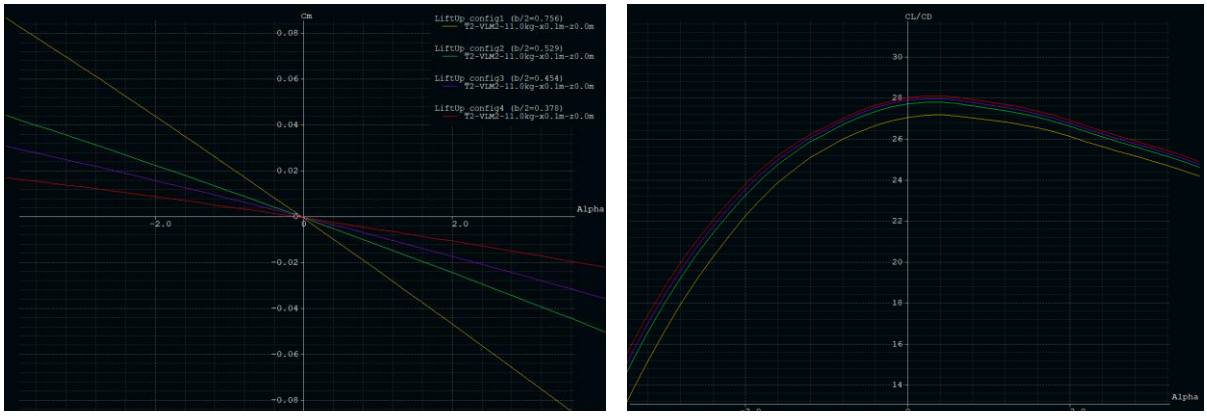

Figure 9: Tail surfaces comparison

We decided to adopt a completely movable surface for two main reasons:

- This solution doesn't create a surface discontinuity that affects the aerodynamic performance of the tail due to the clearance between the fixed surface and the control surface
- With this solution we can easily change the tilt angle of the tail and thus reduce the risk of an incorrect alignment of the tail surface due to the construction tolerances

The team then proceeded to verify static directional and lateral stability. To meet the static directional stability requirements, an aircraft must have a positive yaw rigidity, as expressed by the following inequality:

$$C_{N\beta} = \frac{\partial C_N}{\partial \beta} > 0$$

Generally speaking this requirement is met by all airplanes that have a vertical stabilizer, we analysed the aircraft in XFLR5 and we saw that C_N is a linear function of β, so $C_{N\beta}$ was calculated to be 0,0325.

The requirement to meet to have static lateral stability is that the aircraft has a negative roll rigidity, as expressed by the following inequality:

$$C_{l\beta} = \frac{\partial C_l}{\partial \beta} < 0.$$

This condition is achieved with the dihedral effect of the aircraft, the simplest way to create a dihedral effect is to give a dihedral angle to the wing. For this reason, we imposed a dihedral angle upwards of 2° to the outer wing sections. Again we analysed the configuration in XFLR5, and C_l was a linear function of β, so $C_{l\beta}$ was calculated to be -0,0181.

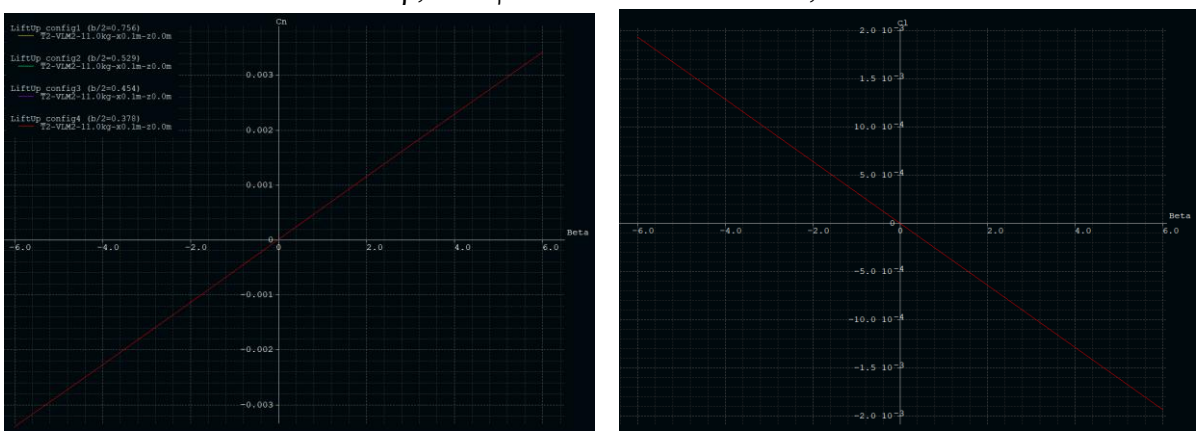

Figure 10: Roll and yaw moment coefficients

After that we decided to give a semi-elliptic plan to the tip of the tail in order to increase the aspect ratio (from $AR_{V/2} = 2{,}82$ it become $AR_{V/2} = 3{,}65$), in particular we decided to maintain the same tail surface of the rectangular tail ($S_{V/2}$=0,073m^2), so the final plan view of the tail is represented below

Coefficient of drag calculation

We proceeded to calculate analytically the wing's drag coefficient during take-off ($C_{D,takeoff}$) and cruise ($C_{D,cruise}$), then we compared the results with the analysis of wing + tail configuration in XFLR5. In particular, the drag coefficient is given by two factors:

- *zero-lift* drag coefficient ($C_{D,0}$)
- induced drag coefficient ($C_{D,i}$)

To calculate $C_{D,0}$ we relied on the empirical relation found in Jan Roskam's *Airplane Aerodynamics and Performance*:

$$C_{D,0} = R_{wf} \cdot R_{LS} \cdot C_{wf} \cdot [1 + L' \cdot (\frac{t}{c}) + 100 \cdot (\frac{t}{c})^4] \cdot \frac{S_{wet}}{S}$$

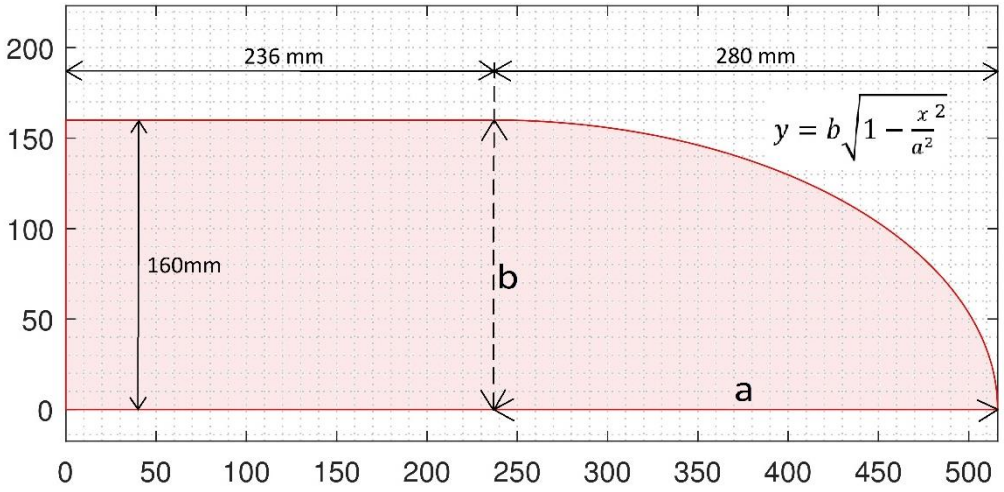

Figure 11: Final shape of the tail

Where the viscous drag C_{wf} was calculated with the next equation

$$C_{wf} = \frac{0{,}455}{(\log_{10}\mathrm{Re})^{2{,}58} \cdot (1 + 0{,}144 \cdot M^2)^{0{,}58}}$$

The *zero-lift* drag coefficient calculated is $C_{D,0}$=0,0123.

To calculate the induced drag coefficient, we used the classic Prandtl's formula:

$$C_{D,i} = \frac{C_L^2}{\pi \cdot e \cdot AR}$$

Where the Oswald factor *e* were calculated with the next equation from Raymer's *Aircraft Design: A Conceptual Approach*, valid for airplanes with no wing sweepback:

$$e = 1{,}78 \cdot (1 - 0{,}045 \cdot AR^{0{,}68}) - 0{,}64 = 0{,}7309$$

Using the value of $C_{L,cruise}$ previously found we calculated $C_{D,i}$=0,0142. By adding this value to $C_{D,0}$we obtained the coefficient of drag in cruise condition $C_{D,cruise}$=0,0242.

This value is ≈30% bigger than the one calculated numerically in XFLR5 (using viscous analysis), which is 0,0180.

We also used the same procedure to calculate the takeoff drag coefficient (even if Prandtl's theory doesn't apply at high angles of attack) and we obtained $C_{D,takeoff}$=0,0910, and then from XFLR5 we obtained 0,0820.

Summary of aerodynamic properties

Here is a summary of the aerodynamic parameters calculated for the plane.

$\alpha_{takeoff}$	11,92°	$V_{takeoff}$	11,24 m/s
α_{cruise}	2,08°	V_{cruise}	18,06 m/s
$C_{L,takeoff}$	1,3945	$C_{D,takeoff}$	0,0910
$C_{L,cruise}$	0,5404	$C_{D,cruise}$	0,0242

Here are the geometric parameters of the tail and the main wing:

	MAIN WING	HALF TAIL
Surface $[m^2]$	1	0,073
Span $[m]$	3,317	0,516
Chord $[m]$	0,302	0,160
Aspect Ratio	11	3,65
Dihedral [°]	2 (outer sections)	33,5

Performance analysis

We used the aerodynamic parameters to calculate the power required by the aircraft in equilibrium condition ($L = W$) in function of the airspeed with the following expression

$$P_R = AV^3 + BV^{-1} \text{ with } A = \frac{1}{2}\rho S V^2 C_{D,0} \text{ and } B = \frac{2W^2}{\rho S \pi A R e}$$

then from the motor + propeller performance we calculated the power available as a function of the airspeed and we obtain the following graph:

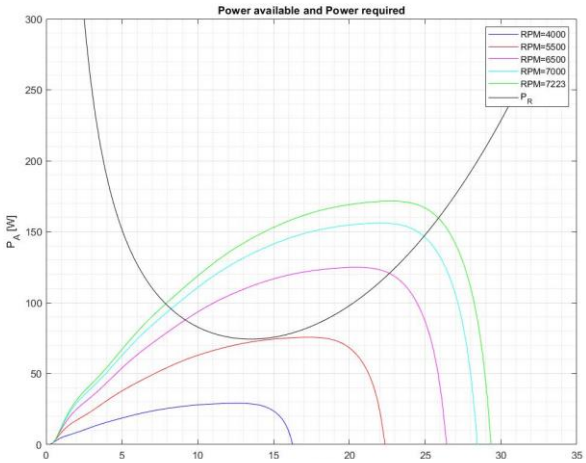

Figure 12: Power and airspeed correlation

We can see that below a minimum value of the motor throttle (5500 RPM) the aircraft cannot take off and that for any particular value of the motor throttle there are two possible flight speeds. We only considered the right solution because of propulsive stability. In the end we can see that the maximum theoretical flight speed is about 25,9 m/s and we used this value to size servo controllers in the worst-case scenario (consider that the value of $C_{D,0}$ was underestimated due to the absence of the fuselage, landing gear, etc, and for this reason the real maximum flight speed would be considerably lower).

Fuselage

Fuselage geometry is the result of an aerodynamic optimization conducted with the aim to reduce the drag of the fuselage. We analysed different fuselages through CFD software however, to reduce the computational cost of the process, we did a 2D analysis and we supposed an axisymmetric fuselage. The geometry was parameterized using Bezier curves, then meshed with Gambit 2.4.6. To solve properly the boundary layer we estimated y+=1 and then we calculated the first cell height. We then analysed it with Fluent 19.2. using k-SST as viscous model. The best results (lower drag) are represented below, and we can see the loss of total pressure and the velocity magnitude around the fuselage.

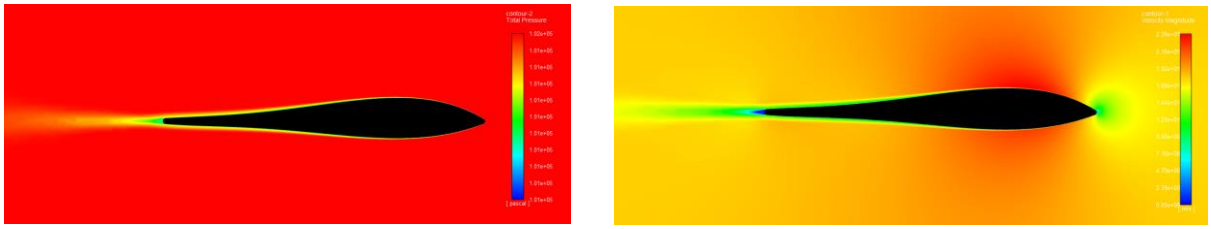

Figure 13: Fuselage CFD results

From this analysis we obtained a rough estimation of the drag coefficient of the fuselage, which resulted equal to 0,0179.

Structural Design

The structure of the aircraft was designed to resist all the expected loads and also to be as close as possible to the aerodynamic model, while accounting for ease of construction.

Wing design

The wing is composed of five pieces, two telescopic carbon longerons (one at 25% and one at 60% of the chord length) and 44 ribs. The central piece contains slots to link the wing to the cargo bay. It's made with a combination of balsa, birch and fir wood, strengthened by carbon reinforcements.

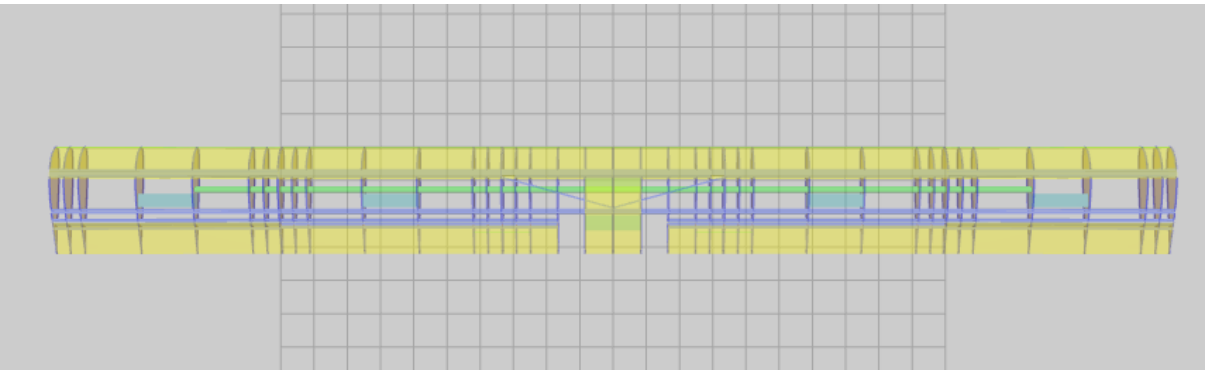

Figure 14: Wing structure top view

The first conceptual design was based on an existing wing provided by the pilot of our team; we also analysed different structures from other exiting wings, but we chose this one as it could be easily studied with classical structural theories. Its features are:

- Two main longerons, one at 25% and one between 60% and 70% of the chord length;
- One diagonal longeron, which links the two longerons, which starts at the wing root and ends at around 200mm from it;
- Ribs held together with wooden battens;
- Balsa wood paneling from the leading edge up to around 25% of the chord along the entire wingspan;
- Balsa wood paneling of the entire airfoil only along the three most central ribs;
- Control surfaces made of ribs covered with two balsa wood panels.

We asked many experienced hobbyists to advise us on the best materials to build the wing with. We chose to use balsa, birch and fir wood for their mechanical properties and ease of use.

Our first hypothesis was to consider wood as an isotropic material. Then, after choosing the number of ribs and a configuration of battens, we estimated the sections of structural elements close to the wing root with classical structural formulas.
Knowing the position of the longerons as a percentage of the chord length, the distance of the longerons from the leading edge and the mechanical characteristics of the wood (taken from "Mechanical Properties of Wood, David W. Green, Jerrold E. Winandy, and David E. Kretschmann"), we calculated the required minimum sections.

This iterative process was implemented within a MATLAB script. The final design was then:

- One longeron at 25% of the chord length, with 20x3mm flanges;
- One longeron at 60% of the chord with a 10x3mm flanges.

We chose to use telescopic longerons after testing a prototype wing with separated ones, which showed us that the load did not distribute along the wing length as evenly as we previously thought.

Tail design

First, we studied the aerodynamic loads acting on the tail, in particular the main load considered is the lift and we considered only the bending moment caused by the lift. We supposed the worst case to be when the tail has an incidence with respect to the airflow of 9° (stall condition of the airfoil) and that it is working at the maximum theoretical airspeed (25,9 m/s). From an XFLR5 analysis we got the following bending moment distribution along the wingspan

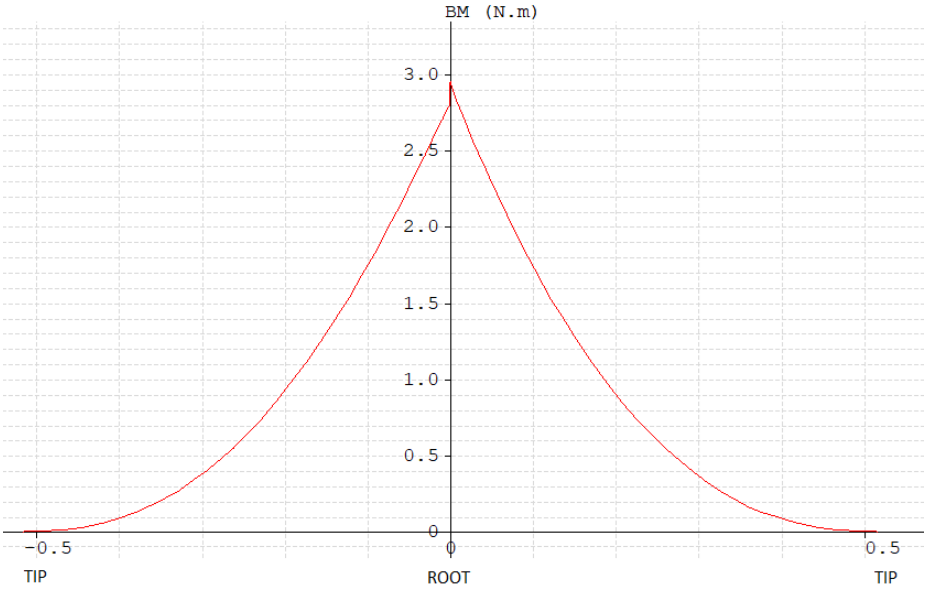

Figure 15: Bending moment along the tail wing

The maximum bending moment is equal to 3 Nm.

We decided to link the tail and the fuselage with a round spar made of unidirectional carbon fiber of ⌀5mm fixed in the fuselage; the tail contains an aluminium tube that houses the round carbon fiber spar and allows the rotation of the tail. Assuming the material of the spar as isotropic we calculated the maximum direct stresses due to bending moment in the round spar section with Navier's formula:

$$\sigma_z = \frac{M_x}{I_{xx}} \cdot y_{max} = 15{,}28Mpa \text{ with } I_{xx} = \frac{\pi R^4}{4} = 4{,}91\text{e} - 10m^4$$

and, assuming a maximum admissible tension of 1,4GPa of the carbon spar (compression-worst case), the beam operates within the admissible working limits.

We placed the round spar at one fourth of the chord length because this point is near the centre of pressure and in this point the pitching moment equals zero, resulting in a smaller torsional moment on the servo controllers. Each half of the tail is composed of 13 ribs. The first one is 1,5mm thick and is made of birch plywood, the other robs are 2mm thick and are made of balsa

wood. All ribs are equally spaced except for the second and the third ones, which are closer in order to have a better load transmission between the ribs and the round spar.

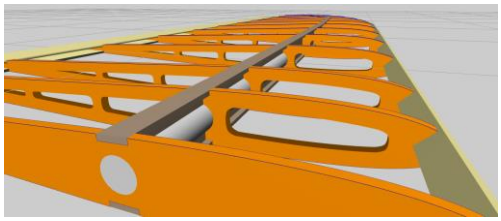

Figure 16: Tail structure, ribs

Balsa ribs also have some lightening holes that have a minimum distance from the edges of 3 mm.

The ribs are connected with an I-section spar that is placed at one fourth of the chord length, which supports the bending moment and to transmits it to the round spar and to the fuselage. The web is made of balsa wood and has a rectangular section, with $t_w = 2mm$ and $h = 4{,}75mm$. Flanges are made of lime wood and have a rectangular section, with $t_f = 1mm$ and $b = 5mm$. Assuming the material of the spar as isotropic we calculated the maximum direct stress in the flanges:

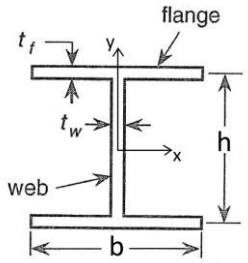

Figure 17: Spar parameters

$$\sigma_z = \frac{M_x}{I_{xx}} \cdot y_{max} = 0{,}30Mpa$$

$$\text{with } I_{xx} = 2\left(\frac{b \cdot t_f^3}{12} + b \cdot t_f \cdot \frac{h}{2}\right) + \frac{h^3 \cdot t_w}{12} = 2{,}377\text{e} - 8m^4$$

and assuming a maximum admissible tension of lime wood of 60MPa the beam operates within the admissible working limits.

The leading edge and the trailing edge are made of balsa wood and contribute to the stiffness of the tail. The tip of the tail is made from a block of balsa wood. In the end the cover skin consists of a cover film.

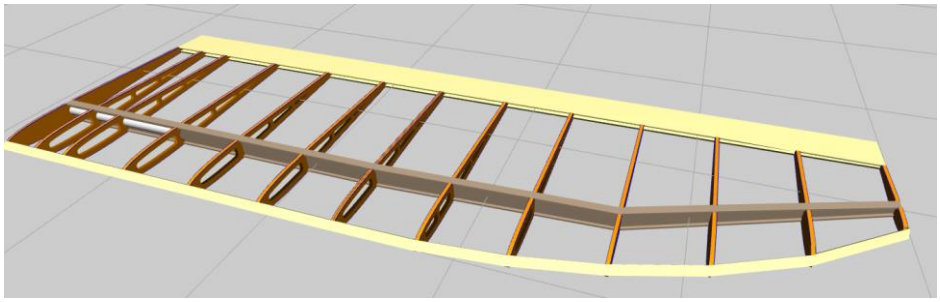

Figure 18: Tail structure

Landing Gear Design

The landing gear has a “taildragger” configuration, with two main wheels in front of the centre of gravity and an auxiliary wheel at the tail. The front piece is a leaf spring structure, while the back wheel is mounted on a torsional spring.

We chose the taildragger configuration as it provides more propeller clearance, has low drag and weight and allows the wing to generate more lift for rough-field operation than other types of gear; the taildragger landing gear was also the preferred layout of our pilot. On the other hand, this type of landing gear can cause an unstable landing and requires the pilot to handle the aircraft with care.

To start, we determined the geometrical configuration of the landing gear from the constraints showed on the picture on the next page:

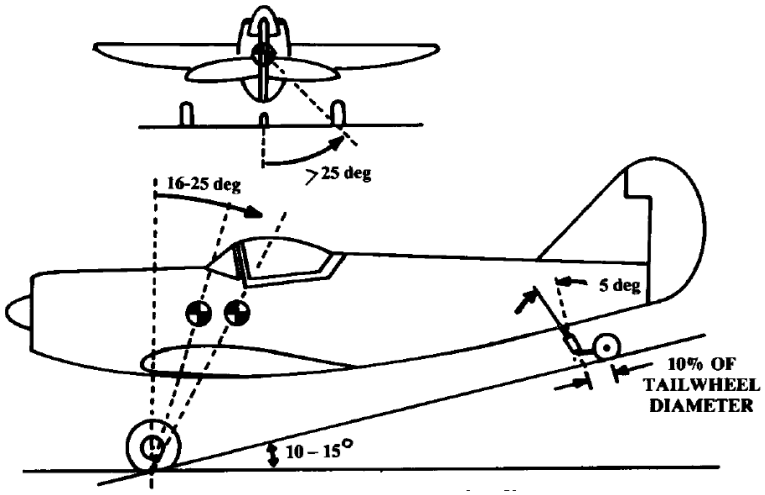

Figure 19: Taildragger constraints

Knowing the fuselage length and the centre of gravity position it's easy to get the position of the longitudinal wheels as $lm = 0{,}1m$ and ln $= 0{,}82m$, where lm is the distance between main gear and c.g. and ln is the distance between rear gear and c.g.
The position of the vertical wheels is determined imposing a tail-down angle of 12° and by considering an arbitrary rear gear length, that we chose to be $8cm$ at maximum in this case. From this we get the main wheels vertical distance of $28cm$.
The turnover angle is set to 45° for constructive ease and for deflection allowance during impact with the ground.

Figure 20: Front gear CAD design

For the front gear piece, we opted for the steel leaf spring or solid-spring design due to its

reliability, simplicity and low aerodynamic drag for non-retractable gear. A landing load factor N is used to represent the total effect of both static and dynamic loads on the structure, so the analysis reduces to a merely static case in which the force acting on gears is N times the aircraft weight. N is then defined by the sum of all forces on the gear divided by the mass and in our case is set to 3.

The main gear leg is then modelled as a tapered cantilever beam that must be able to withstand a load equal to three times the MTOW (maximum take-off weight) with a safety factor $SF = 2$on material's yield for maximum stresses, and the chosen material is Al7075-T6, an aluminum alloy that is particularly elastic, light and has a high yield stress. The sizing process is made with the aid of an iterative process, and results are validated through finite element analysis.

Geometry	Value
length	0.2687
thickness	0.0040
root width	0.0343
tip width	0.0200
mass	0.0820

Stress-strain	Value
displacement	0.0474
stroke	0.0335
static stroke	0.0089
maximum stress	2.5134e+08

Figure 21: front gear, iterative process results

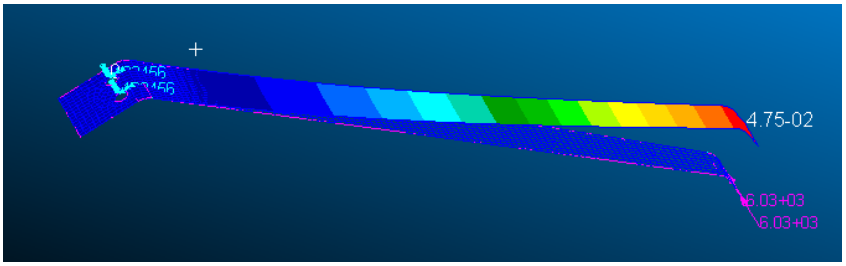

Figure 22: Front gear, FEM analysis results

The rear gear consists of a small torsion spring with a small wheel. On our first prototype we used a skid for both its simplicity and its low aerodynamic drag, but this idea has been rejected due to tail-soil drag troubles when fully loaded.

The sizing then consisted in the determination of a proper torsion spring to be used, following a theoretical model that allows to predict the stress-strain behaviour under a certain loading condition. For simplicity the load is set to three times the static load on the rear wheel, that from static equilibrium is equal to 11% of the MTOW, and the maximum allowable displacement is set to $1.5cm$roughly. The chosen material is spring steel, since it's the most suitable metal for springs due to its high elasticity. Again, the sizing process results were confirmed through finite element analysis.

Figure 23: Rear gear CAD design

property	value
wire diameter	0.0020
maximum stress	6.9549e+08
displacment	0.0145
stroke	0.0072
stiffness	906.8503

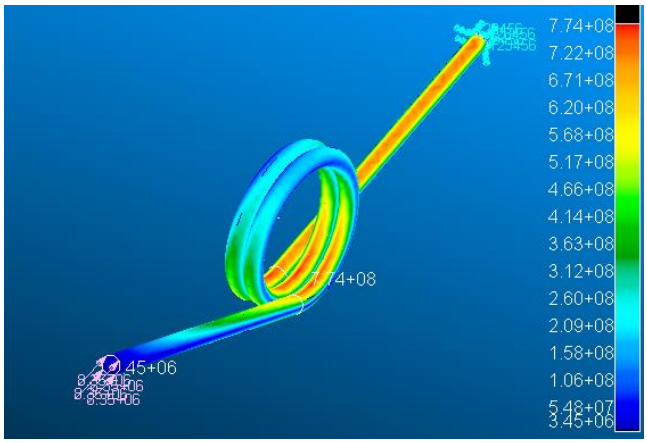

Figure 24: Rear gear analysis results

Cargo Bay design

The cargo bay is shaped like a parallelepiped with a missing face and its made with a carbon fiber composite material. The payload is inserted into the hole on the side of the box with a sled.

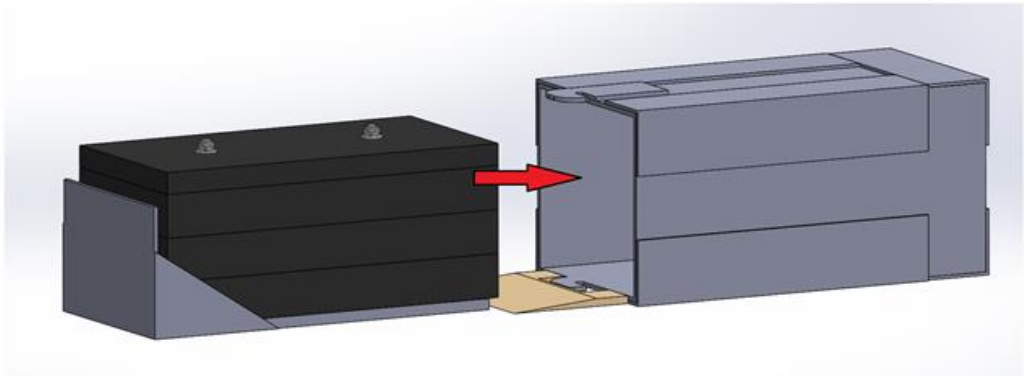

Figure 25: Cargo bay CAD design

Two carbon rods are fixed to the sled to keep the plates in position. The plates are held in place with nuts and washers to avoid their displacement.

The sled is kept in place inside the box with a pin. To allow an easier insertion we designed a simple ramp that guides it into the box.

The cargo bay is placed inside the fuselage under the wing to ensure that the centre of gravity of the plane is not affected by the weight of the payload. The fuselage has an opening through which the sled and the pin can be put in place.

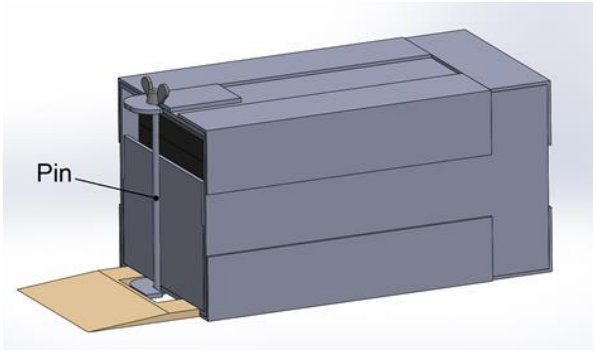

Figure 26: Closed cargo bay

Electronic systems

As for electronics, we chose a Graupner Tx/Rx system, as it can control two different receiver modules; one is located inside the fuselage and controls the engine and the two tail servo controllers, while the other one is placed inside the wing and controls the aileron and flap servo controllers. This allows us to connect the whole wing electronics with just a single JR connector, easing links between wing and fuselage.

The servo controllers were sized as follows:
For the flaps we supposed they would never be deployed at speeds higher than 60 Km/h (16,7 m/s) and that their maximum angle, when landing, is 30°; the equivalent torque was calculated with XFLR5 and is 0,3793 Nm (3,793 Kg*cm).
For the ailerons we supposed the worst-case scenario to be when the speed is at its theoretical maximum of 93 Km/h (25,9m/s), corresponding to an angle of attack of 2.1°, and with 30° of deflection; the equivalent torque in this case is 0,7279Nm (7,279 Kg*cm).
For the tail we considered at maximum 9° of deflection, corresponding to a torque of 0,585 Nm (5,96Kg*cm)
The servo controllers were chosen accordingly to these results.

Production

Landing gear

The construction process of the main gear started with the cutting of an aluminium sheet at the corresponding nominal length, which was then bent on a matrix that gave it its final and correct shape. In order to fix the landing gear to the fuselage, we made two holes with a drill press; first we punched the aluminium, then we enlarged the actual holes until the correct diameter was reached. After the supporting frame was complete, wheels were fixed through a hub with special care to not cause any rubbing.

For the rear gear, we heated a spring steel rod and bent it over a metal pipe to shape the torsion spring that composes the gear. It was then bent at its end to accommodate the small wheel, kept in place by two nuts, and finally fixed to the fuselage.

Fuselage

The fuselage is made of an epoxy resin and carbon fibers composite material. The main steps to accomplish the production process are summarized as follows.

From the SolidWorks 3D model of the fuselage we extracted equally spaced transverse and longitudinal sections, which we edited in order to build a wooden frame of the fuselage with them, which would become the master for the lamination mould. We then laser-cut the fuselage sections from 2 mm birch wood sheets, assembled them to a reference structure, and filled the empty spaces between the cut-outs with polyurethane foam. We then coated the frame applying and sanding a first layer of polyester body filler, then coated it with multiple layers of epoxydic primer, and lastly a final layer of epoxydic gel coat. The master was then polished to a perfect glossy finish, ready to use for the mould construction.

To support the master, we built a structure with the inclusion of two PVC flanges aligned with the longitudinal plane of symmetry of the fuselage. This auxiliary structure has been used to ease the subsequent layering process of the laminae, which are the bulk of the actual mould. The object was split into two halves correspondingly to half of the overall fuselage length. The layering process to laminate the mould begins by applying a release agent onto all the exposed surfaces of the master and the flanges, and then a layer of epoxydic gel coat. After that, takes place the actual hand lamination of the laminae constituting the mould, made of glass fiber and epoxy resin layers. Once the mat was thoroughly wetted out, the lamina was stippled to ensure that any air pockets were driven out; this last procedure has been repeated multiple times to ensure enough structural integrity of the mould. The same process has been done for the second mould.

The last step is the actual lamination of the fuselage, utilizing the previously built mould by means of a standard vacuum assisted resin infusion moulding process. We left the part to fully cure and, the day after, we de-moulded and refined it cutting the waste material, leaving the

finished carbon fiber fuselage.

The laminate that makes up the fuselage is composed by a first set of the following three laminae:
LAYER 1: TeXtreme® Carbon fabric (plain)
LAYER 2: Carbon non-crimp fabric ST (Unidirectional-UD)
LAYER 3: CARBOWEAVE (+/- 45°).

A second set of layers is arranged in a specular way to the aforementioned ones in order to achieve a symmetric stacking sequence of the laminae constituting the final laminate.

The first lamina is a plain weave spread tow carbon fiber fabric pattern, suited to respond well to an overall range of solicitation; in particular, the spread tow design should improve the buckling response of the structure.
The second lamina is designed to improve resistance to the bending solicitation of the fuselage, which represents the majority of the load cases bore by the structure.
The third lamina is designed to account for the torsion solicitation of the structure.
A fourth lamina of unidirectional carbon fabric pattern (same as layer 2) is layered transversally to the fuselage (+/-90°) to strengthen only the joint areas of the wings and the landing gear.

Wing

The main wing was built with three different types of wood and some carbon reinforcements. The ribs were designed with CAD software and cut from balsa and birch wood sheets with a CNC laser machine. To keep them in place while gluing them to the battens we first built a rack-like structure, specifically designed for our wing. The racks also help reduce the buckling of the battens. One wing piece at a time, we glued the battens to the ribs with epoxy glue in such a way that would not generate any residual tensions, which could induce an unwanted buckling of the wing piece (as can be seen on the pictures on the next page).

Once the battens were all in place, we glued the tip of the wing before gluing the 1mm balsa wood paneling with cyanoacrylate glue. Servo controllers were screwed inside some predisposed internal boxes.
The control surfaces are made of two balsa wood sheets ribbed with the same geometry of the wing they are linked to. To strengthen the fastening of the servo controllers, we inserted a small piece of wood right where the servo controller lever is fixated.

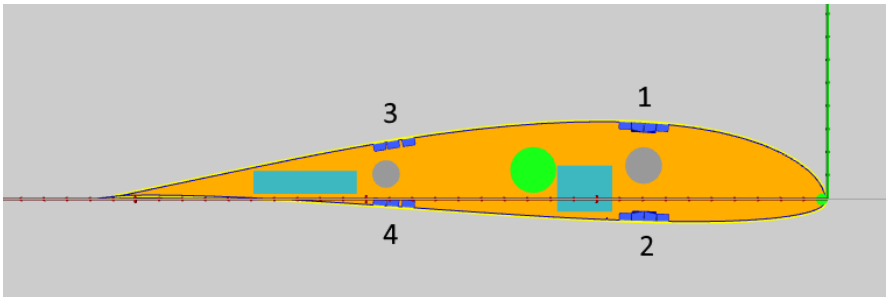

Figure 27: Recommended gluing sequence

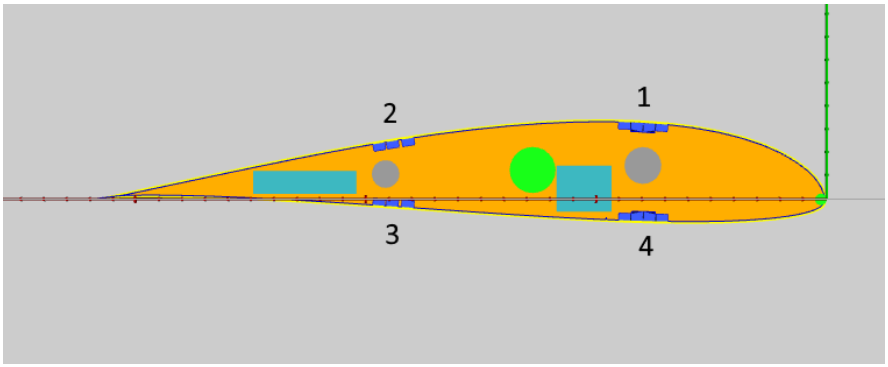

Figure 28: Not recommended gluing sequence

Cargo bay

The cargo bay is mainly made of epoxy resin and carbon fibers composite material.
The inner section of the box is made of five carbon fiber sheets glued together by epoxy resin. At the edges of the box are placed L-shaped section bars to ensure structural rigidity and continuity along the box surface.
The sled is made in the same way, with different shaped composite panels glued together to achieve the desired shape. At the base of the sled we drilled two holes to fix two carbon fiber rods, serving as guides for the payload plates, to which ends we glued small threaded bars in order to fix the plates with nuts.
The pin that prevents the sled from sliding when inserted is a simple steel rod threaded on one end and a washer soldered to the other one.

Payload Prediction

The weight-density formula and its graphical representation are the following:

$$m_{PL} = 2{,}214m^{-3} \cdot \rho + 2{,}785kg$$

where $\rho$is the air density in kg/m^3 and m_{PL} is the payload mass measured in kg.

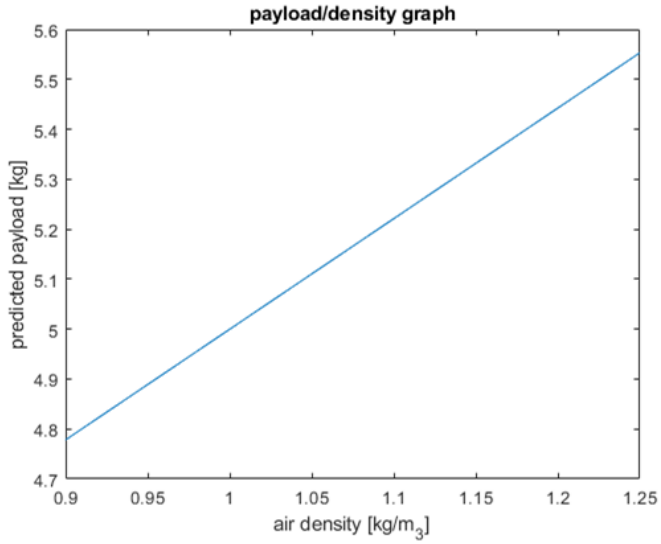

Figure 29: Payload prediction graph

Using the results of aerodynamic design and structural design, from which we derived the aerodynamic parameters and an estimation of the aircraft's total mass, we wrote a MATLAB code to find the maximum weight the plane can lift in various flight conditions and patterns. The code considers the constraints given by the competition's regulations and various ambient parameters such as air density, runway's friction et cetera.

The aircraft's maximum weight corresponds to the abscissa of the highest intersection point between the red line and any one of the coloured surfaces. As expected, the critical flight segments are lift-off (the green one) and ascent (the blue one). By computing the results for various atmospheric density values, we found expected total masses (to which we subtracted the expected mass without payload) and their corresponding densities. We then used a least-square interpolation between the two sets of data to find the requested *a* and *b* coefficients.

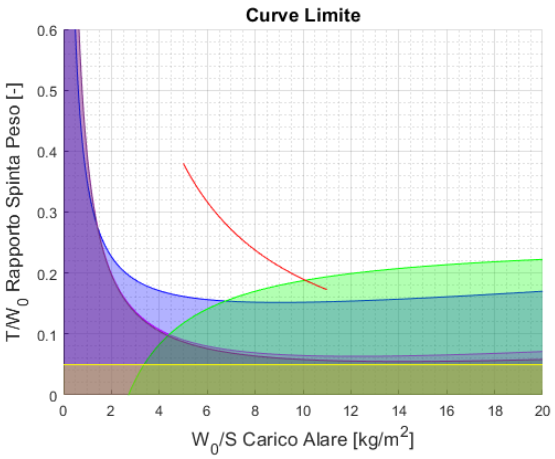

Figure 30: Flight pattern constraints

A more precise and specialized model is currently in the works; this new model should take into account more external parameters, leading to better results.

Tests on the prototype

Once our prototype was built we conducted flight tests to validate our models and to find potential issues. The first flights were used to calibrate the movement of control surfaces from the pilot's feedback.

We also experimented with different approaches to both lift-off and landing. We found significant differences on the behaviour of the aircraft depending on the control surface configuration used.

With that settled, we proceeded to conduct more technical measurements using both onboard and ground sensors. We prepared an empty template, which we filled before and after each flight with both quantitative (atmospheric parameters, lift-off distance, etc) and qualitative (pilot's impressions, flight overall performance, etc) data.

Each flight was filmed from the ground for later analysis. We also did some stall tests with an onboard camera in order to better understand the airflow around the wing.

Figure 31: Stall test, onboard camera

We intend to continue testing both our prototype and our final aircraft, using the first one as a guinea pig for riskier and more invasive trials.

Outlook

As this is our first participation in the Air Cargo Challenge we did not have any previous practical experience in designing and building an aircraft and, as such, we did not take any exceptionally risky design choices.

Now, having built some experience in both design and construction, we intend to improve our aircraft with more complex and performing features.

Regarding aerodynamics, we want to study the feasibility of winglets and vortex generators. We also intend to work on a retractable landing gear which would dramatically improve the overall aerodynamic performance.

As for structures, we would like to switch to a carbon fiber laminate wing, which could result in a lighter structure.

When the ACC competition will be over, we intend to show our work to CUAMM, a non governative organization of volunteer doctors located in Padua, which could use our drone to deliver medical supplies to African towns and villages unreachable by common means.